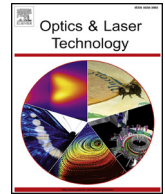




ELSEVIER

Contents lists available at ScienceDirect

## Optics and Laser Technology

journal homepage: [www.elsevier.com/locate/optlastec](http://www.elsevier.com/locate/optlastec)

Full length article

## Effect of heat input on the subgrains of laser melting deposited Invar alloy

Xiaohong Zhan<sup>a,\*</sup>, Chaoqi Qi<sup>a</sup>, Junjie Zhou<sup>a</sup>, LiJun Liu<sup>b</sup>, Dongdong Gu<sup>a</sup><sup>a</sup> College of Material Science and Technology, Nanjing University of Aeronautics and Astronautics, Nanjing 211106, China<sup>b</sup> Ningbo Institute of Technology, Zhejiang University, Ningbo 315100, China

## HIGHLIGHTS

- Invar alloys have been prepared using a laser melting deposition process.
- The subgrains orientation changed in the DL.
- This paper shows different subgrain morphology under different heat input.
- There is a dimension discrepancy of remelted and non-remelted subgrains.

## ARTICLE INFO

## Keywords:

Microstructure evolution  
Quantitative subgrain size  
Subgrain orientation  
Invar alloy  
Laser melting deposition

## ABSTRACT

Invar alloys are widely used in the aerospace, but their manufacturability and mechanical properties are not well understood when they are employed in additive manufacturing. The laser melting deposition (LMD) technology is utilized to the surface repair of Invar alloys. In this work, the microstructure evolution, quantitative subgrain size, as well as the subgrain orientation are investigated using optical microscopy. Moreover, the effect of partially remelting of successive layers is exhibited. It is explicit that the cellular crystal orientation is strongly influenced by the heat flow which is subject to the scanning direction. Considering to the basic laws of Invar alloy microstructure evolution during LMD process, the relations between heat input and produced subgrain characteristics are further elucidated. The results show that a slight increase of  $\lambda$  from 4.4  $\mu\text{m}$  to 5.2  $\mu\text{m}$  at the function of heat input varied from 98.6 J/mm<sup>2</sup> to 114 J/mm<sup>2</sup>. Moreover, it was notable that a reverse change in the dimension discrepancy of remelted and non-remelted subgrains occurred with two kinds of heat input.

## 1. Introduction

Invar alloys discover their successful utilization as molds of carbon fiber due to their superior mechanical properties in cryogenic environment and similar thermal expansion coefficient with composites [1–4]. Nevertheless, some problems occurred when the Invar alloy components serviced, including increases in porosity, crack formation, other defects in the course of welding assembly. In addition, the material and manufacture of these components are excessively costly [5,6]. It is therefore indispensable to extend the service life of these components through the application of repairing technologies.

Generally, the high-quality molds cannot be repaired by traditional overlaying techniques, i.e. arc welding, because of its inferior quality, which is a result of large heat-affected zone (HAZ). Compared with traditional overlaying techniques, the laser melting deposition (LMD) technology provides a solution to allow a small dilution rate, dense microstructure, and high-strength metallurgical bonding with the

substrate. As an emerging repairing technique, LMD has already attracted considerable attention in aviation [7]. The LMD technology is analogously attractive for complicated components because, by transferring from a computer-aided design (CAD) model, the powders injected from a coaxial nozzle are fed directly into a melt pool generated by a heat source, accurately leading to the powders and substrate surface melting and solidification layer by layer [8,9]. Thus, the LMD offers an opportunity to create Invar alloy components with high density, accuracy and excellent performance by melting and solidifying metal powders into three-dimensional structures [10]. Meanwhile, the LMD technology provides benefits on repairing the high-quality Invar alloy molds which are applied in aerospace.

After recent years of research, a variety of alloys manufactured by LMD with different constituent have been studied, including Ni-based superalloy [11,12], titanium alloy [13,14], aluminium alloy [15] and stainless steel [16]. Bobbio et al. [17] combined experimental characterization and computational analysis to investigate a material

\* Corresponding author.

E-mail address: [xiaohongzhan\\_nuaa@126.com](mailto:xiaohongzhan_nuaa@126.com) (X. Zhan).<https://doi.org/10.1016/j.optlastec.2018.08.013>

Received 28 May 2018; Received in revised form 7 August 2018; Accepted 9 August 2018

0030-3992/ © 2018 Published by Elsevier Ltd.

graded from Ti-6Al-4V to Invar 36, creating innovative application of the LMD technology. It has reported that laser melting deposited rail repairs were fabricated by Lai et al. [18] In their study, the effects of scanning direction, preheating and post heat treatment on microstructure and mechanical properties were presented, which demonstrated that the properties were tremendously correlation with the LMD parameters.

Invar alloys are of increasing scientific interest since their discovery of the superior low thermal expansion properties [19,20]. Recently, considerable improvements on Invar alloy manufacture have been reported. Harrison et al. [21] validated that the unique low thermal expansion property of Invar was retained when processed using selective laser melting (SLM) technique. Prior to Harrison's progress, the microstructure and properties of selective laser-melted Invar 36 was performed by Qiu et al. [22]. It was elucidated that process parameters were liable for the surface microstructure. Moreover, it was concluded by Zhan et al. [23] that the process parameters played an important role in the forming size of deposited layer and the HAZ width of deposition structure. Overall, the laser melting deposited Invar alloys are infrequent, so that the relations among heat input and microstructure evolution are far from being completely established. Thus, there is merit in attempting to explore the subgrain characteristic on the basis of the aforementioned researches.

In this work, the LMD method was adopted to fabricate the surface layers of Invar alloys, focusing more attention on the microstructure evolution, measurable subgrain sizes and the subgrain orientation. The smart idea of quantitative research on LMD process makes it a candidate for the accurate repairing of Invar alloy molds. As the main investigation objectives of the paper, the relations between heat input and subgrain characteristics were further established.

## 2. Experiment

### 2.1. Experimental materials

The base powder (BP) used in the current study is Invar alloy powder treated by a plasma rotation electrode process (PREP), which has the size range from 50  $\mu\text{m}$  to 150  $\mu\text{m}$ . Rectangular Invar alloy plates with the dimension of 40 mm  $\times$  30 mm  $\times$  19 mm are applied as the base material (BM) during the LMD experimental process. The plates are grit blasted to improve laser absorptivity and degreased with acetone to remove contaminants prior to deposition. The chemical compositions of substrate and deposited powder are shown in Table 1.

### 2.2. Experimental equipment

The experimental configuration is composed of an IPG YLS-6000 laser machine with a rated output power of 6 kW, a coaxial XSL-ST powder feeder, a Six-axis linkage robot and an atmosphere control system. Parts of the experiment equipment are shown in Fig. 1(b–e). The laser melting deposition processing is illustrated schematically in Fig. 1(a). In this process, a high-power laser is focused on a substrate to create a molten pool. Synchronously, a metal powder is continuously injected into the melt pool with argon gas as the shielding gas, and subsequently, the melt pool is solidified as deposition layer.

### 2.3. Experimental methods

Experimental parameters are selected via preliminary experiments to ensure a low level of porosity in the LMD process. Final process parameters utilized in this paper are provided in Table 2, showing the different heat input. The same experimental parameters are selected for the comparative analysis of single-layer and multi-layer deposition process. More specifically, with regard to the samples produced by multi-layer multi-pass experiment, the layer number is 4 and the pass number is 36. On the basis of determined parameters, the schematic

and results of single-layer sample and multi-layer multi-pass samples are as shown in Fig. 2. During the process, all the samples are isolated from the environment using a fixed chamber which is continuously flushed with argon at a flow rate of 15 l/min. Meanwhile, the oxygen level is measured by the oxygen analyzer which is connected with the chamber. The argon is also supplied to the powder feeder at a flow rate of 10 l/min to serve as a carrier gas for powder delivery into the melt pool.

Metallographic specimens are etched with two types of solution, one of which contains 30% HCl, 10% HNO<sub>3</sub> and 60% H<sub>2</sub>O. The other is 4% nital. To reveal the size, distribution and orientation of subgrains, the samples are examined using optical microscopy (OM) and scanning electron microscopy (SEM).

## 3. Results and discussion

### 3.1. Subgrain characteristics of single-pass samples

The transverse section and longitudinal section images with different magnification of the single-pass samples are observed by OM, as shown in Figs. 3–5. It should be noteworthy that the LMD parameters tailored in this paper fabricate the sample with good formability containing neither cracks nor bonding error at the interface between deposited layer and substrate. Notwithstanding porosity in deposited layer (DL) can be eliminated efficiently under protecting gas, a small minority of pores exist in the deposit. As LMD is an extraordinary rapid solidification process, the heating and cooling speeds are virtually high, leading to a high possibility of shielding gas entrained in the process [24]. Therefore, it is extremely crucial to investigate heat input during the LMD process.

Figs. 3(a) and 4(a) show the microstructure of single-pass samples from the BM to DL. It is noticed that the BM completely consist of the single-phase austenite grains. The region in which coarse equiaxial grains are observed between the BM and DL is recognized as the HAZ. The boundary between HAZ and DL is fusion line, highlighted by a yellow<sup>1</sup> dotted line. Fig. 3(a) reveals that the cross-section microstructure of Case 1 (lower heat input) is composed of two regions, columnar grains and equiaxed grains. It is obvious that columnar grains grow epitaxially from the substrate at the bottom part. Meanwhile, the bottom grains consist of elongate cellular crystals with dissimilar direction and equiaxed cellular crystals, which are shown in Fig. 3(c and d). Three straight lines with a length of 100  $\mu\text{m}$  are marked to measure the subgrain sizes. It is calculated that the average dendrite spacing of subgrains at the bottom part is approximately 4.4  $\mu\text{m}$ , the value of which is measured through the Eq. (1).

$$\lambda = \frac{L}{n} \quad (1)$$

With L and n, respectively, being the length of the test line and the number of counted cellular crystals. Fig. 3(e) represents that the morphology of the top part is typically equiaxed grains, of which the equiaxed cellular structure of varying sizes is full. It is worth to mention that the very few secondary dendrites have been detected through OM method. Therefore, the subgrain research in this paper properly revolves around cellular crystals.

On the longitudinal section view, it is found in Fig. 3(f) that microstructure of Case 1 is mainly composed of columnar grains which grow competitively. As implied in the detailed image, the transformation from equiaxed cellular crystals to the elongate is an important feature in the grains. From the bottom to the top of the DL, a gradual transition of the subgrain orientation is explicit. It is manifest that the laser scanning direction and the grain orientation of substrate play both

<sup>1</sup> For interpretation of color in Figs. 3 and 4, the reader is referred to the web version of this article.

Download English Version:

<https://daneshyari.com/en/article/11003686>

Download Persian Version:

<https://daneshyari.com/article/11003686>

[Daneshyari.com](https://daneshyari.com)